

## Electron states in *n*-type inversion layers with periodic microstructure

Ulrich Wulf

*I. Institut für Theoretische Physik der Universität Hamburg, Jungiusstrasse 9,  
2000 Hamburg 36, Federal Republic of Germany*

(Received 24 October 1986)

The electron states of an inversion electron layer with a periodic density modulation are calculated self-consistently in a mean-field approximation. It is shown that drastic changes in the electronic properties occur as the modulation and the electron density are varied. In particular the electron-electron interaction has strong effects on the localization of the inversion electrons. The transition from localized to extended behavior is quite abrupt as a function of the electron density.

### INTRODUCTION

The fabrication of metal-oxide-semiconductor (MOS) systems with microstructured gates has recently become possible. These systems allow the study of inversion electron layers which are closely bound to the oxide-semiconductor interface and show a periodic density modulation along one direction parallel to the oxide-semiconductor interface. In such systems both transport experiments<sup>1</sup> and spectroscopic experiments<sup>2,3</sup> have been reported. Since screening in a two-dimensional electron gas is less effective than in three dimensions, consideration of the electron-electron interaction is very important for the interpretation of these experiments.<sup>4</sup> At present, theories are only available for systems with strong modulation,<sup>5-7</sup> where the system can be split into independent electron channels with quasi-one-dimensional character. However, experiments have also been carried out in the opposite limit in which the microstructure only leads to a weak modulation of the electron gas. In this paper we give the results of self-consistent calculations of the electronic states over the entire modulation range. Exchange-correlation effects are neglected.

### THE EFFECTIVE POTENTIAL FOR AN INVERSION ELECTRON

The effective potential  $V$  for an inversion electron is determined by the gate potential, the interaction with other inversion electrons, the depletion charge, and by the image charges. In mean-field theory, the following equation is to be solved:

$$\Delta V = -\frac{4\pi e^2}{\kappa}(n + n_d), \quad (1)$$

where  $\kappa$  is the static dielectric constant of the solid.  $n$  and  $n_d$  are the inversion electron and depletion charge densities, respectively. The actual gate structure leads to complicated periodic boundary conditions at the gate. A Fourier transformation of the effective potential in the direction of the modulation shows, however, that the behavior of the inversion electrons is mainly effected by the lowest harmonic. Higher harmonics are strongly weakened within the oxide and will be assumed negligible

for a sufficiently thick oxide [see Eqs. (4) below]. Therefore we may write the boundary conditions at the gate as

$$V(x, z = -D_{ox}) = V_G + V_M \cos(K_0 x), \quad (2)$$

where  $D_{ox}$  and the  $x$  and the  $z$  directions are defined in Fig. 1 and  $K_0$  is the wave vector of the microstructure.  $V_G$  is the constant potential at the gate which determines the average number of electrons per unit area.  $V_M$  is the amplitude of the first Fourier component of the superimposed microstructure potential and characterizes the degree of modulation. In addition the boundary conditions at the gate and at the semiconductor interface determine the image charges. Taking the Fourier transform of the Poisson equation [Eq. (1)] and inserting

$$n(x, z) + n_d(x, z) = \sum_r [n_r(z) + n_{d,r}(z)] \times \exp(-iq_r x), \quad (3a)$$

$$V(x, z) = \sum_r V_r(z) \exp(-iq_r x), \quad (3b)$$

$$q_r = rK_0, \quad r = 0, \pm 1, \pm 2, \dots \quad (3c)$$

we obtain for the indicated boundary conditions the following solution for  $r \neq 0$ :

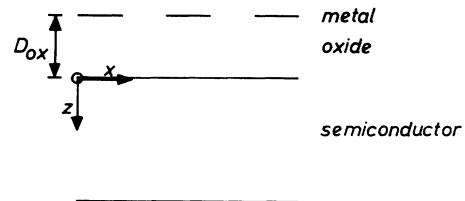


FIG. 1. Schematic geometry of the microstructured MOS system.

$$V_{r \neq 0}(z > 0) = \frac{\epsilon V_M}{\epsilon \cosh(|q_r| D_{\text{ox}}) + \sinh(|q_r| D_{\text{ox}})} \frac{1}{2} \delta(|q_r|, K_0) \exp(-|q_r| z) + \frac{2\pi e^2}{\kappa_{\text{sc}}} \int_0^\infty n_r(z') G_r(z', z) dz' + \frac{2\pi e^2}{\kappa_{\text{sc}}} \frac{\sinh(|q_r| D_{\text{ox}}) - \epsilon \cosh(|q_r| D_{\text{ox}})}{\sinh(|q_r| D_{\text{ox}}) + \epsilon \cosh(|q_r| D_{\text{ox}})} I_r \exp(-|q_r| z), \quad (4a)$$

with

$$G_{r \neq 0}(z', z) = \frac{\exp(-|q_r| |z' - z|)}{|q_r|}, \quad (4b)$$

$$I_{r \neq 0} = \frac{1}{|q_r|} \int_0^\infty \exp(-|q_r| z') n_r(z') dz', \quad (4c)$$

where  $\kappa_{\text{ox}}$  and  $\kappa_{\text{sc}}$  are the static dielectric constants of the oxide and the semiconductor and  $\epsilon = \kappa_{\text{ox}}/\kappa_{\text{sc}}$ . The first term on the right-hand side of Eq. (4a) is the external gate potential, which rapidly becomes small with increasing  $q_r$ . The second term gives the mutual interaction of the inversion electrons. This term does not contain the effect of the discontinuity in the dielectric constants, which is explicitly exhibited in the third term as an effective image potential. The depletion charge only enters in the  $q_r = 0$  part of the effective potential since the acceptors in the depletion zone are totally ionized and give thus a homogeneous potential. A modulation of the depletion charge only occurs at the transition to the bulk and therefore contributes little to the higher potential harmonics for the same reasons as given above. Thus we obtain for  $r = 0$ , according to Ref. 4,

$$V_{r=0}(z > 0) = \frac{4\pi e^2}{\kappa_{\text{sc}}} \left[ \left( N_{\text{depl}} + \frac{N_s}{2} \right) z + \frac{\bar{z}}{2} - \frac{1}{2} \int_0^\infty n_{r=0}(z') |z - z'| dz' \right], \quad (5)$$

where  $N_{\text{depl}}$  and  $N_s$  are the depletion and inversion charges per unit area averaged over one period.  $\bar{z}$  is defined by

$$\bar{z} = \int_0^\infty z n_{r=0}(z) dz.$$

### SELF-CONSISTENT EQUATIONS

The calculation is carried out in effective-mass approximation with a diagonal mass tensor at  $T = 0$ . Because of the translational invariance along the channel, and the periodicity in the  $x$  direction, we may write for the wave function

$$\Psi_{k,v,j,k_y} = \exp(ik_y y) \exp(ikx) u_{k,v,j}(x, z). \quad (6)$$

Here the index  $j$  relates to the subband splitting due to the triangular inversion potential and denotes the number of nodes perpendicular to the interface.  $u_{k,v,j}$  is the periodic part of a Bloch function in the  $x$  direction. Using the effective potential of Eqs. (4) and (5) and neglecting exchange and correlation effects one obtains the well-known self-consistent equations ( $\hbar = 1$ ) for  $u_{k,v,j}$ ,

$$\left[ -\frac{1}{2m_z} \frac{\partial^2}{\partial z^2} - \frac{1}{2m_x} \left[ \frac{\partial^2}{\partial x^2} + 2ik \frac{\partial}{\partial x} - k^2 \right] + [V(x, z) - E_{k,v,j}] \right] u_{k,v,j}(x, z) = 0, \quad (7a)$$

with

$$\Delta V = -\frac{4\pi e^2}{\kappa} (n + n_d),$$

$$n(x, z) = \int_{\text{occ}} \frac{dk}{2\pi} \sum_{j,v} N_{k,v,j} |u_{k,v,j}(x, z)|^2, \quad (7b)$$

$$N_{k,v,j} = \frac{2g}{\pi} [2m_y (E_F - E_{k,v,j})]^{1/2}. \quad (7c)$$

Here  $m_y$  is the effective electron mass in the  $y$  direction,  $E_F$  is the Fermi energy, and  $g$  is taking into account a possible valley degeneracy.  $N_{k,v,j}$  results from the  $k_y$  summation over all occupied states with

$$E_{k,v,j} + k_y^2 / 2m_y \leq E_F. \quad (7d)$$

The computations were performed by expanding all functions with respect to a basis system of normalized products of free waves in the  $x$  direction and shifted Airy functions in the  $z$  direction (see Ref. 4).

### RESULTS

In studying microstructured systems one has to distinguish between two limiting cases with respect to the relation between the triangular inversion potential and the microstructure potential. While the former is responsible for the subband splitting, the latter gives rise to the formation of Bloch bands in the  $x$  direction. If both potentials are of comparable size, both of these splittings mix and thus give a very complicated energy spectrum. Since we are mainly interested in the influence of the microstructure, we have chosen a fairly steep inversion potential in order to keep the subbands well apart. For numerical computations we use the parameters of a SiO<sub>2</sub>-Si MOS structure with Si in (100) orientation ( $\kappa_{\text{sc}} = 11.5$ ,  $\kappa_{\text{ox}} = 3.9$ ,  $g = 2$ ,  $m_z = 0.916m_0$ , and  $m_x = m_y = 0.19m_0$ ). The inversion electron density is taken to be small enough so that only the lowest valley is occupied. The oxide thickness and the reciprocal periodicity are chosen to be  $D_{\text{ox}} = 26$  nm and  $K_0 = 2\pi/200$  nm =  $3.14 \times 10^5$  cm<sup>-1</sup>, respectively.

Figure 2 shows the position of the bottoms  $E_b = E_{k=0, v=1, j}$  of the first three subbands in dependence on  $N_s$ . Here the external potential [see first terms in Eqs. (4a) and (5)] is fixed at  $V_M = 20$  mV and  $N_{\text{depl}} + \frac{1}{2} N_s = 3.5 \times 10^{11}$  cm<sup>-2</sup>. The dashed line gives in comparison the values of a corresponding homogeneous system. The zero of energy is taken at the lowest band; in

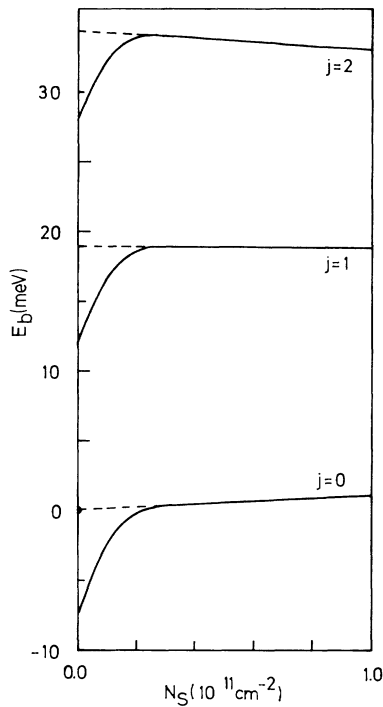


FIG. 2. Energy of subband bottoms vs electron density. The external potential is determined by  $N_{\text{depl}} + \frac{1}{2}N_s = 3.5 \times 10^{11} \text{ cm}^{-2}$ ,  $V_M = 20 \text{ mV}$  (solid line) and  $N_{\text{depl}} + \frac{1}{2}N_s = 3.5 \times 10^{11} \text{ cm}^{-2}$ ,  $V_M = 0 \text{ mV}$  (dashed line).

the latter case at  $N_s = 0$ .

The results show that at high densities the values of  $E_b$  are nearly the same in homogeneous and microstructured systems. This occurs in spite of a considerable density modulation as can be seen from Fig. 3. For low densities,  $E_b$  is distinctly smaller in the microstructured system and very sensitive to changes of the electron density. Figure 4

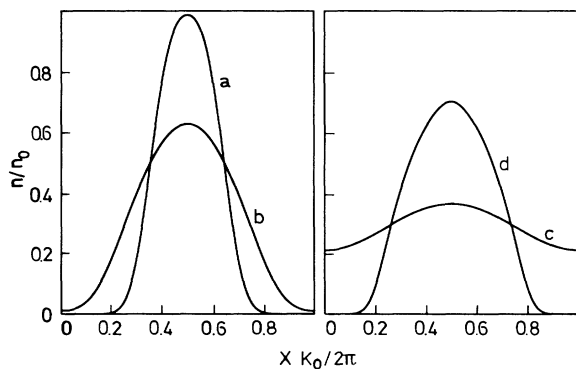


FIG. 3. Normalized modulation of the electron density in the  $x$  direction. The  $z$  value is taken at the maximum. With  $N_s$  and  $N_{\text{depl}}$  in units of  $10^{11} \text{ cm}^{-2}$  and  $V_M$  in mV the following parameters were used: (a)  $N_s = 0.1$ ,  $N_{\text{depl}} = 3.45$ ,  $V_M = 20$ ; (b)  $N_s = 0.25$ ,  $N_{\text{depl}} = 3.375$ ,  $V_M = 20$ ; (c)  $N_s = 1.0$ ,  $N_{\text{depl}} = 3.0$ ,  $V_M = 20$ ; (d)  $N_s = 1.0$ ,  $N_{\text{depl}} = 3.0$ ,  $V_M = 100$ .

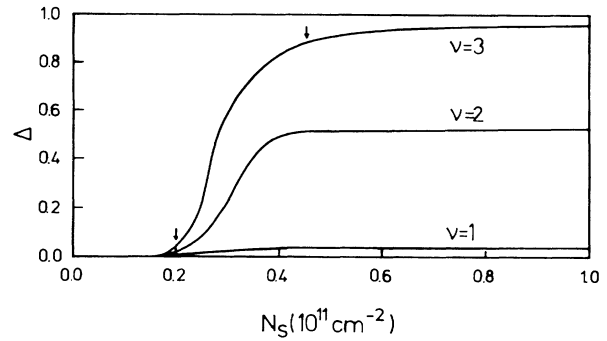


FIG. 4. Width of the Bloch band and energy gaps represented by  $\Delta$  (see text) vs  $N_s$ . The parameters correspond to the case of the solid line for  $j = 0$  in Fig. 2.

illustrates the width of the Bloch bands and the gaps belonging to the lowest subband of Fig. 2. Here the quantity  $\Delta = W / (E_g + W)$  is shown, where  $W$  is the Bloch band width and  $E_g$  is the gap above the corresponding band. It is seen that  $\Delta$  approaches a constant close to 1 for  $\nu = 3$ , indicating that these electrons are nearly free. In contrast the gap is preserved in the lower Bloch bands through the entire range shown, which demonstrates their bound character.

The system's behavior exhibited in Fig. 2 may be explained by the fact that the microstructure potential is effectively screened at high densities. Thus in this case the influence of the microstructure potential on  $E_b$  nearly vanishes. It is evident that the electrons in the lowest lev-

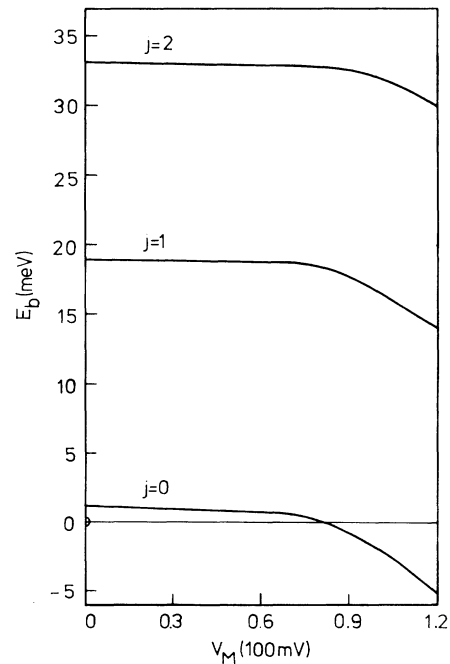


FIG. 5. Energy of the subband bottoms vs the amplitude of the microstructure potential with  $N_s = 10^{11} \text{ cm}^{-2}$  and  $N_{\text{depl}} = 3 \times 10^{11} \text{ cm}^{-2}$ .

els contribute most of the screening of the microstructure potential. Once these "valence" levels are occupied the higher bands show practically free-electron behavior. This is exhibited in Fig. 4 for the three lowest Bloch bands. While all of them are practically localized for small densities, the screening effect leads to a delocalization of the third band at  $\nu=3$  at high densities.

Turning to the influence of the amplitude of the microstructure potential, Fig. 5 shows the subband bottoms  $E_b$  for fixed  $N_s = 10^{11} \text{ cm}^{-2}$  which corresponds to the right edge of Fig. 2. It is evident that the number of electrons necessary for screening the potential depends on the

amplitude of the microstructure. This is clearly exhibited in Fig. 5 where the levels do change at first very little when the microstructure potential is increased. Around  $V_M = 70 \text{ mV}$  the screening breaks down and the energy levels start to react to a further increase of  $V_M$ . That the lowest band is affected most strongly is due to the fact that these states lie closest to the surface in a region where the decay of the microstructure potential is weak.

#### ACKNOWLEDGMENT

The author is grateful to Professor H. Heyszenau for valuable discussions.

---

<sup>1</sup>A. C. Warren, D. A. Antoniadis, and H. I. Smith, *Phys. Rev. Lett.* **56**, 1858 (1986).

<sup>2</sup>U. Mackens, D. Heitmann, L. Prager, J. P. Kotthaus, and W. Beinvoogl, *Phys. Rev. Lett.* **53**, 1485 (1984).

<sup>3</sup>U. Mackens, D. Heitmann, and J. P. Kotthaus, *Surf. Sci.* **170**, 346 (1986).

<sup>4</sup>T. Ando, A. B. Fowler, and F. Stern, *Rev. Mod. Phys.* **54**, 437 (1982).

<sup>5</sup>S. E. Laux and F. Stern, *Appl. Phys. Lett.* **49**, 91 (1986).

<sup>6</sup>A. C. Warren, D. A. Antoniadis, and H. I. Smith, *IEEE Electron Device Lett.* **EDL-7**, 413 (1986).

<sup>7</sup>W. Y. Lai and S. Das Sarma, *Phys. Rev. B* **33**, 8874 (1986).